Immunity, Vol. 15, 751–761, November, 2001, Copyright ©2001 by Cell Press

The Immunological Synapse of CTL Contains a Secretory Domain and Membrane Bridges

Jane C. Stinchcombe, Giovanna Bossi, Sarah Booth, and Gillian M. Griffiths[1]
Sir William Dunn School of Pathology
South Parks Road
Oxford, OX1 3RE
United Kingdom

Summary

Cytotoxic T lymphocytes (CTL) rapidly destroy their targets. Here we show that although target cell death occurs within 5 min of CTL-target cell contact, an immunological synapse similar to that seen in CD4 cells rapidly forms in CTL, with a ring of adhesion proteins surrounding an inner signaling molecule domain. Lytic granule secretion occurs in a separate domain within the adhesion ring, maintaining signaling protein organization during exocytosis. Live and fixed cell studies show target cell plasma membrane markers are transferred to the CTL as the cells separate. Electron microscopy reveals continuities forming membrane bridges between the CTL and target cell membranes, suggesting a possible mechanism for this transfer.

Introduction

Activated CD8 cytotoxic T lymphocytes (CTL) play an important role in destroying tumorigenic and virally infected cells. This killing is highly efficient and involves only transient interaction between CTL and target. Movies of living cells have shown that CTL are serial killers capable of destroying targets within times as short as 2–10 min (Matter, 1979; Rothstein et al., 1978; Sanderson, 1976; Zagury et al., 1975) and then killing further targets only 6 min later (Poenie et al., 1987). Upon target cell recognition, CTL rapidly polarize their microtubule organizing center (MTOC), Golgi complex (Geiger et al., 1982; Kupfer and Singer, 1989), and lytic granules (LG; Yannelli et al., 1986) toward the target cell. These granules, which contain the proteins capable of destroying the target cell (Page et al., 1998), fuse with the CTL plasma membrane at the site of contact and release their contents toward the target (Peters et al., 1989).

Recent studies have described an "immunological synapse" formed by CD4 T lymphocytes and their antigen-presenting cells (APCs), which involves rearrangement of cell surface proteins into a distinct topological organization (reviewed in Davis and van der Merwe, 2001; Delon, 2000; Delon and Germain, 2000). Signaling molecules cluster in a central supramolecular activation complex (cSMAC) surrounded by adhesion molecules, such as LFA-1, in the peripheral SMAC (pSMAC; Monks et al., 1998). The finding that this organization is stable and can be maintained for several hours has led to the suggestion that the synapse is important in providing sustained T cell receptor (TCR) signaling required for CD4 function (Grakoui et al., 1999). Since CTL do not require sustained signaling for their immediate effector functions of degranulation and target cell death, it has not been clear whether an immunological synapse is formed by these cells and where within such a structure granule secretion might occur.

More recently, a synapse has been described between B lymphocytes and APCs, leading to acquisition by B cells of antigenic membrane proteins from the target (Batista et al., 2001). Transfer of antigen from target to CTL during killing (Huang et al., 1999; Hudrisier et al., 2001) has also been shown to render the CTL increasingly susceptible to fratricide (Huang et al., 1999), suggesting that this may be an important mechanism in downregulation of CTL responses. We therefore decided to examine the site of CTL and target interaction, and ask whether an immunological synapse was formed, what determines the site of degranulation delivering the lethal hit, and by what mechanisms membrane proteins might be transferred during this interaction.

Results

CTL Polarize Their Lytic Granules and Trigger Target Cell Apoptosis Rapidly after Cell Contact

To determine the time scale of events in CTL-target cell interaction, we exploited the fact that the lytic granules of CTL are modified lysosomes, often referred to as secretory lysosomes (Burkhardt et al., 1990; Peters et al., 1991). These organelles can be labeled in vivo using LysoTracker Red DND-99, a cell-permeant dye which accumulates and fluoresces in acidic compartments in live cells. CTL derived from C57BL/6 mice and loaded with LysoTracker Red DND-99 were mixed with P815 target cells expressing the EYFP-tagged palmitoylation domain of neuromodulin, which labels the plasma membrane (P815-pEYFP-mem), and the live cells were followed in vivo using confocal video microscopy. Figure 1 illustrates single images from the time-lapse video shown in Supplemental Movie S1 at http://www.immunity.com/cgi/content/full/15/5/751/DC1, which illustrates the events that follow establishment of a tight contact between the two cells (defined as $t = 0$; Figure 1A). Within the first minute of interaction, granules visible within this plane of focus begin to move toward the contact site (Figures 1A–1C). Intriguingly, by 90 s (Figure 1D), an indentation has appeared in the target cell membrane directly opposite one of the CTL granules, and this marks the region where the rest of the granules subsequently accumulate (Figure 1F). This is strikingly shown in the animated version (Supplemental Movie S1), where the granules can be seen streaming around both sides of the nucleus toward this single point at the contact site. By 3 min of CTL-target cell interaction, granule polarization is complete, and already by 4–5 min, the membrane of the target cell shows signs of membrane blebbing, characteristic of apoptotic cell death (Figures 1G and 1H). Although the target is clearly dying after 5 min of CTL-target cell interaction, several of the granules have

[1] Correspondence: gillian.griffiths@path.ox.ac.uk

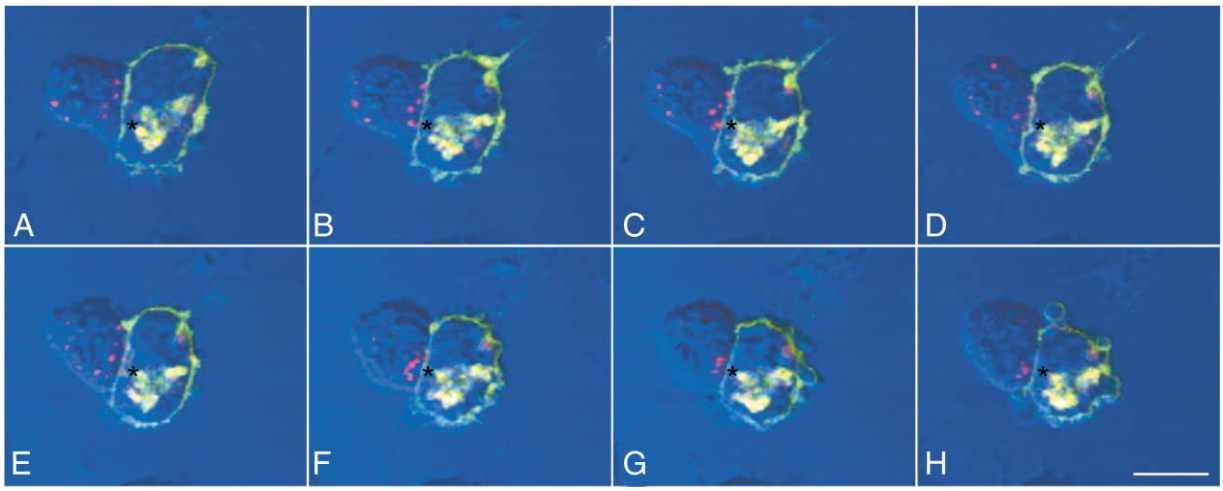

Figure 1. Lytic Granule Polarization and Target Cell Death Occur Rapidly after CTL-Target Cell Contact

Selected images taken from the live cell time-lapse video microscopy shown in Supplemental Movie S1. CTL (left) were loaded with LysoTracker Red DND-99 (red) and added to P815 target cells (right) expressing pEYFP-mem (green). Images taken at 0 (A), 40 (B), 60 (C), 90 (D), 120 (E), 180 (F), 240 (G), and 300 (H) s intervals after the establishment of cell-cell contact are shown. Nomarski differential interference contrast (blue) and 1 μm confocal fluorescence (red and green) images are shown superimposed for each time point. Asterisks indicate the point in the membrane to which the LG polarize (F–H), where an indentation in the target cell plasma membrane appears (D). Note that in (G) and (H), the target cell membrane shows blebbing characteristic of apoptotic cell death. The scale bar represents 10 μm.

not released their fluorescent content, and even after 14 min (Supplemental Movie S1), labeled granules are still visible in the CTL. This suggests that CTL do not need to exocytose all of their granules for a target cell to be killed. Despite the fact that some variation in the time taken to kill targets was seen between CTL derived from different strains of mice, the results described above were remarkably reproducible. Granules consistently focused toward a point at the contact site where an indentation appeared in the target cell membrane.

Talin Accumulation Precedes Granule Polarization

We previously showed that in CTL-target cell conjugates in which the granules were polarized, talin was present in a ring-like structure at the contact site membrane, suggesting reorganization of membrane proteins was occurring along the contact site (Stinchcombe et al., 2001). In order to establish the relationship between granule polarization and reorganization at the contact site, we examined conjugates for markers of polarization and synapse formation. CTL and P815 target cells were mixed and plated onto microscope slides for 30 min, a time which allows the cells to adhere and significant numbers of CTL to find their targets. Conjugates were then fixed and stained with antibodies against the soluble lysosomal hydrolase cathepsin D, the *cis*-Golgi 58 kDa protein (p58), and tubulin, to identify the granules, Golgi complex, and microtubule cytoskeleton, respectively. Since CTL encounter their targets at different points during the 30 min incubation, different cells within a single sample are trapped at different stages of interaction and granule polarization. These stages are shown in Figures 2A–2E. In the absence of target cells (Figure 2A), the MTOC and Golgi complex have a perinuclear localization and the granules are dispersed along microtubules throughout the cell. As shown previously (Geiger et al., 1982; Kupfer and Dennert, 1984; Kupfer et al., 1985, 1986), granule polarization is preceded by reorientation of the MTOC followed by the Golgi complex to the point of contact between the two cells (Figure 2B). The granules polarize, clustering behind and around the MTOC and Golgi complex (Figure 2C). The MTOC and Golgi complex shift closer to the contact site, and the granules align tightly with the contact membrane on the other side of the MTOC/Golgi complex cluster (Figure 2D). Figure 2E shows the dramatic decrease in the total fluorescent signal given using antibodies against granule content in tightly polarized cells compared with unpolarized cells (Figure 2A), consistent with the secretion of granule content during target cell killing.

To study the relative time scales of granule polarization and markers of synapse formation, we looked at the distribution of talin at different stages of granule polarization (Figures 2F–2J). In the absence of P815 targets, antibodies against talin give a very weak cytosolic staining with very little signal associated with the CTL membrane (Figure 2F). However, significant amounts are recruited to the cytosolic face of the membrane across the contact site upon interaction with target cells and before either the CTL MTOC or granules have polarized (Figure 2G; 8% of conjugates). This membrane-associated talin is rapidly reorganized into a ring-like structure, and occurs after MTOC but before granule polarization (Figure 2H). In 17% of conjugates, the central hole lacking talin is very broad and the granules are unpolarized (Figure 2H). In 65% of conjugates, the granules are polarized and the talin hole is narrower (Figure 2I). Interestingly, the size of this hole varies between conjugates (Figures 2I and 2J), and may reflect the section viewed or different strengths of TCR recognition. In 10% of conjugates with a talin hole, virtually all granzyme A labeling was absent, suggesting all granules were secreted.

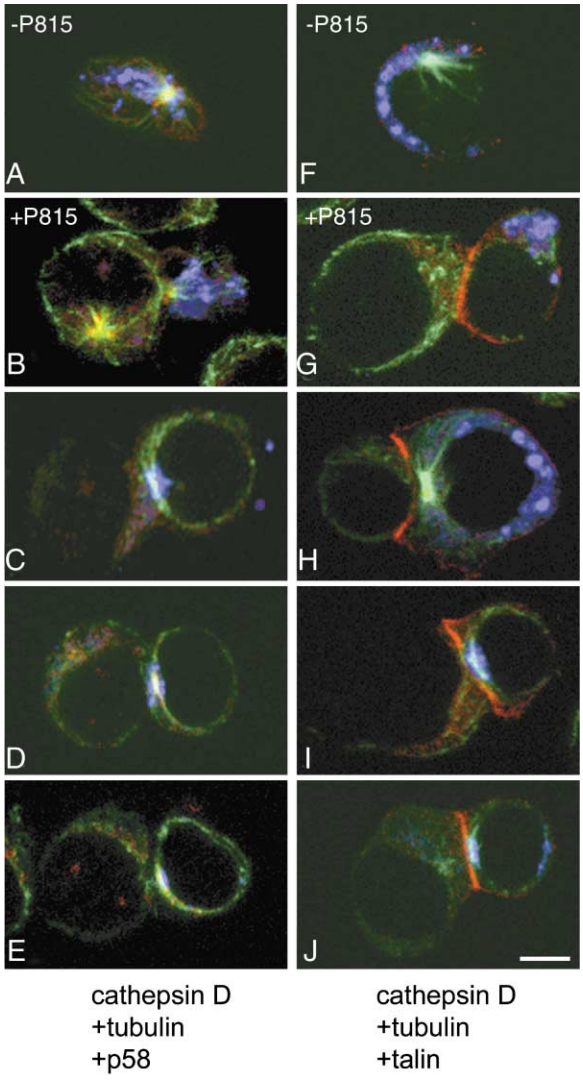

Figure 2. Early Morphological Events Occurring in the CTL upon Target Cell Recognition

Confocal images showing CTL mixed with P815 target cells stained with antibodies against cathepsin D (blue), tubulin (green), and either *cis*-Golgi protein, p58 (A–E), or talin (F–J) (red). CTL which have not encountered targets are shown in (A) and (F). CTL (right) target (left). The scale bar represents 4 μm.

An Immunological Synapse Forms in CTL upon Target Cell Interaction

To investigate whether an immunological synapse similar to that characterized between CD4 cells and their APCs is formed between CTL and their targets, we examined the distribution of several additional surface and cytoplasmic proteins shown to have distinct localizations at the CD4-APC contact site.

In CD4 cells, talin is recruited to the CD11a-CD18 (LFA-1) complex, which accumulates in the pSMAC of the immunological synapse and surrounds the cSMAC-containing signaling molecules such as Lck and PKC-θ (Monks et al., 1998). As shown in Figures 3A–3F, in the absence of targets when talin is dispersed throughout the cytoplasm of CTL (Figure 3A), LFA-1 (identified using an antibody against the LFA-1-specific CD11a subunit) is distributed around the CTL membrane (Figure 3B). Little overlap is seen between these two markers (Figure 3C). Upon contact with the target, CD11a (Figure 3E), like talin (Figure 3D), becomes concentrated at the contact site, forming an outer ring (Figure 3F) resembling the pSMAC described upon CD4 interaction with APCs (Monks et al., 1998).

Low levels of Lck are already associated with the CTL plasma membrane before interaction with a target, while PKC-θ is entirely cytosolic (data not shown). However, high levels of both proteins become concentrated at the contact site upon target cell recognition, where they form a sharp, distinct patch within the CD11a adhesion ring (Figures 3G–3L). The phosphatase involved in the activation of Lck, CD45, is largely excluded from the immunological synapse (Figures 3M–3O).

Overall, the arrangement of proteins at the CTL synapse resembles that described for CD4 T lymphocytes, with proteins involved in TCR signaling forming a central cSMAC within a pSMAC containing the adhesion molecules. However, two subtle differences are observed. First, in all cases, the patch of signaling proteins at the CTL contact site membrane is asymmetric and concentrated to one side of the hole in the LFA-1 ring, leaving a gap between the signaling and adhesion protein domains (e.g., Figures 3I and 3L). This gap is consistently seen with all the signaling and adhesion molecules tested. Second, significant, but lower levels of PKC-θ are also present in the pSMAC (Figures 3J–3L). Very little PKC-θ is observed at the membrane outside the contact site. One interesting point is that while antibodies can gain access to proteins within the contact site of fixed conjugates, those which are known to block interactions in vivo (e.g., blocking antibodies to CD18; data not shown) cannot do so.

Granule Secretion Occurs between the Signaling and Adhesion Domains

To determine where granule exocytosis was occurring within the synapse, CTL-target cell conjugates were labeled with antibodies against markers of the granules, pSMAC and cSMAC, and analyzed by confocal microscopy. Three-dimensional (3D) and z axis image reconstruction was used to visualize the contact site (Figure 4; Supplemental Movies S2 and S3). Like talin (e.g., Figure 2G), Lck and PKC-θ were found to accumulate at the CTL-target cell contact site before the granules polarize (data not shown) and remain there during polarization. Both single (2D) confocal sections (x-y; Figure 4A) and 3D image reconstruction (x-y-z; Figure 4B; Supplemental Movies S2, S4, and S5; Supplemental Figure S1) show the granules (blue) align to one side of the LFA-1 (green) hole, and appear to be "inserted" in a gap between the signaling protein (Lck; red) and adhesion domains. Z axis image reconstruction of the samples in the plane of the contact site was then used to give an en face view of the proteins at the CTL immunological synapse (Figure 4C). This shows clearly that the signaling protein region (Lck; red) and granule contents (cathepsin D; blue) are organized into two distinct, nonoverlapping zones within the adhesion ring (LFA-1; green). Quantitation of 40 conjugates in which Lck was accumulated at

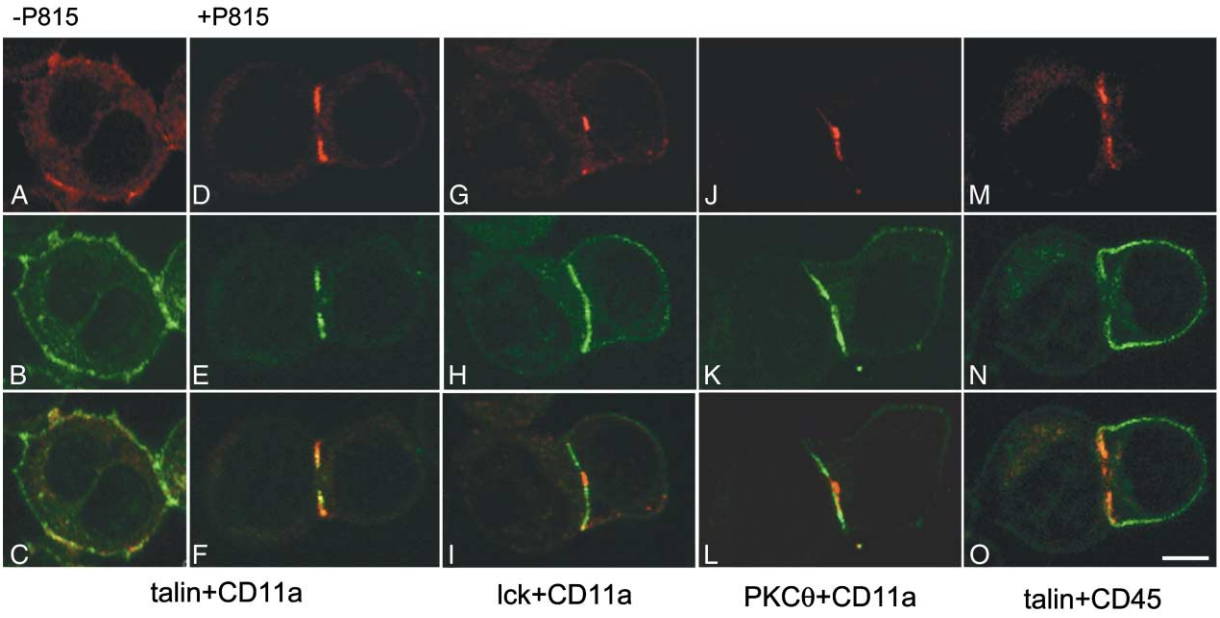

Figure 3. Signaling and Adhesion Molecules Occupy Distinct Domains within the CTL-Target Contact Site Membrane

Confocal images showing samples prepared as in Figure 2 and incubated with antibodies against CD11a (green, [B–O]), talin (red, [A, C, D, F, M, and O]), Lck (red, [G and I]), PKC-θ (red, [J and L]), and CD45 (green, [N and O]). (A–C) show CTL which have not yet encountered a target; (D–O) show CTL (right)-target (left) conjugates at a stage after talin ring formation.

Note that in (G–L), that although both Lck and PKC-θ concentrate within the CD11a ring, the signal is to one side of the CD11a hole, leaving a gap in the labeling of the contact site. The scale bar represents 4 μm.

the contact site revealed that granules were polarized behind Lck in 42.5%, "inserted" next to Lck in 40%, and completely secreted in 12.5% of cases. This is also very striking in samples labeled with granzyme A (green), Lck (red), and an antibody against actin (blue), which only stains at the periphery of the contact site. Since the adhesion ring is unlabeled in these samples, it appears as a black ring (Figures 4D–4G; Supplemental Movies S3, S6, and S7; Supplemental Figure S1). Intriguingly, in cells with highly polarized granules, granule content signal can often be detected on the target cell side of the Lck domain, suggesting that it has been secreted from the CTL (Figure 4G). Taken together, these results show that the granules of CTL are secreted at a defined position of the immunological synapse and therefore suggest that the synapse structure may play a role in secretion. They also indicate that signaling protein organization is maintained during granule exocytosis and therefore that the signaling and secretory functions of the CTL can occur separately and simultaneously.

Granules Secrete at a Cleft between the CTL and Target Cell Membranes

Our studies suggest that the granules move to a specific domain at the contact site for exocytosis. What defines this as the site at which secretion occurs? To investigate events at the contact site in more detail, CTL were incubated with fluid phase HRP overnight to load the secretory lysosomes, and then mixed with P815 target cells, fixed, and analyzed by electron microscopy. In the absence of P815 targets, the centrioles of the CTL MTOC are in the central, perinuclear region of the cell surrounded by elements of the Golgi complex (Figure 5A). The granules are dispersed throughout the cell (see Figures 2A and 2F), and none are visible within the 4.0 × 4.0 μm field surrounding the MTOC shown in this image. Figure 5B shows MTOC polarization toward a "point contact" (arrow). The Golgi stacks and other cytoplasmic organelles including the mitochondria and granules appear to be streaming toward the polarized MTOC. Other samples show extensive areas of tight membrane contact between the CTL and target with the MTOC, Golgi, and mitochondria polarized, while the granules are distant from the plasma membrane (Figure 5C).

Consistent with the immunofluorescence data (Figures 2C, 2D, 2H, and 2I), the granules become increasingly clustered around the Golgi complex and then move to become tightly aligned with the CTL membrane (Figure 5D). Interestingly, granules line up with the contact site on either side of the Golgi complex but are usually excluded from the region immediately opposite the MTOC (e.g., arrows in Figures 5D and 5E). In conjugates where the granules are tightly apposed to the plasma membrane, gaps are seen between the two cell membranes immediately opposite the sites of granule alignment (Figure 5D, arrowheads), and in some cases, the granules appear to be releasing their content into these gaps (Figure 5E). The areas of CTL membrane with no aligned granules directly opposite the MTOC and Golgi complex and either side of the site of the clustered organelles remain in tight contact with the target cell membrane. Sections taken below the area of membrane interaction opposite the MTOC reveal that these gaps are part of a large "cleft" between the two otherwise tightly associated cell membranes, which often appears as an indentation in the target cell membrane (Figure

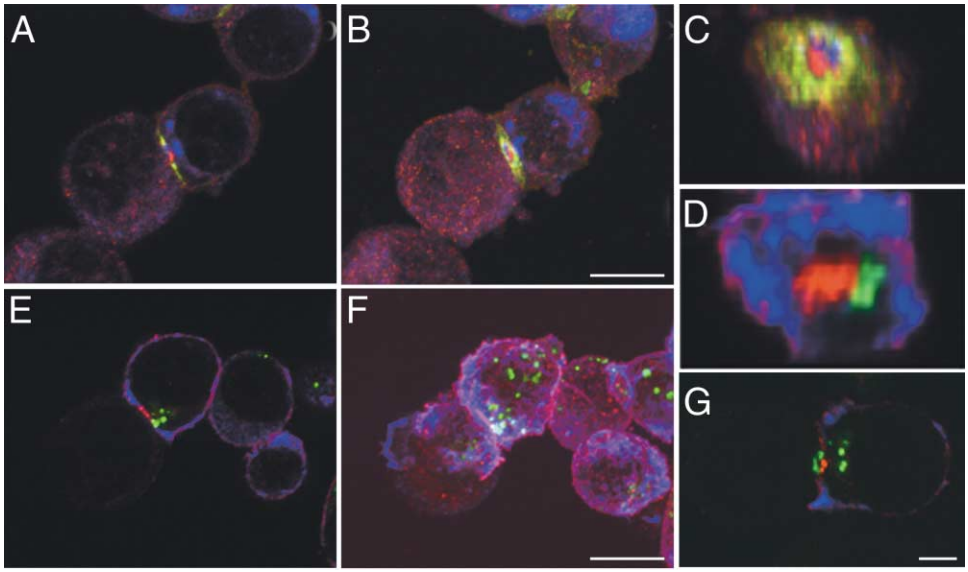

Figure 4. CTL Secretory Lysosomes Insert between the Signaling Molecule Patch and the Adhesion Ring

CTL-P815 target cell conjugates stained with antibodies against Lck (red) and either CD11a (green) and cathepsin D (blue, [A–C]), or granzyme A (green) and actin (blue, [D–G]). CTL and P815 target cells are shown on the right and left, respectively, in (A), (B), and (E–G). Three separate conjugates are shown (A–C, D–F, and G).

(A), (E), and (G) are single confocal sections, (B) and (F) are projected confocal sections taken 0.4 μm apart through the sample (shown as 3D image reconstructions in Supplemental Movies S2 and S3), and (C) and (D) are z axis image reconstructions shown in the plane of the contact site. The lytic granules insert to the side of the signaling protein marker (A, B, E, and F) within the adhesion ring (A and B). (C) and (D) clearly show that the signaling and secretory molecules are distributed into two distinct domains within the adhesion ring (green in [C] and shown by the black ring lacking signal in [D]) at the contact site. Note, especially in (B) and (F), that different stages of granule polarization and secretion are happening simultaneously with some granules already inserted between the signaling patch and adhesion ring while others are still polarizing.

(G) A single confocal section demonstrating granule content protein (green) appearing on the target cell (left) side of the CTL (right) membrane defined by the Lck (red) signal. The scale bars represent 10 μm (A, B, E, and F) and 4 μm (G).

5F). These clefts are consistent with the indentations which form in the target cell membranes opposite the site of CTL granule polarization observed in the live cell studies using P815-pEYFP-mem target cells (Figure 1D).

Images such as that shown in Figure 5E suggest that the cleft marks the site of degranulation. To examine this in more detail, fixed preparations of CTL-P815-pEYFP-mem conjugates were labeled with antibodies against either talin (Figure 6A) or PKC-θ (Figure 6B) to identify the CTL synapse structure, and granzyme A (Figure 6C) and cathepsin D (Figures 6A–6C) to label the granule content. Figure 6 shows that the indentation in the target cell membrane forms opposite the talin hole and to the side of the signaling proteins PKC-θ (Figure 6B) and Lck (data not shown), and that the granule content proteins are present within the cleft. Intriguingly, although both granzyme A and cathepsin D can be detected within these clefts, we often find that they preferentially label with antibodies against granzyme A rather than cathepsin D, even though the granules remaining within the cell may contain both markers (e.g., Figure 6C). Together, these observations support the idea that the cleft represents the site of granule exocytosis and additionally suggest that the granule content accumulates there before entering the target cell. Interestingly, clefts are also observed between the two cell membranes when target cells are conjugated with CTL from *ashen* mice, which lack the small GTP binding protein rab27a and are unable to secrete their granule content (Stinchcombe et al., 2001). This indicates that cleft formation is independent of granule secretion and therefore raises the possibility that the location of these clefts may define the site of exocytosis.

The organization of the molecules and structures at the CTL-target cell interface suggested by our results are summarized in the diagram in Figure 6D. This shows the pSMAC adhesion ring enclosing both a domain containing signaling molecules and a separate domain involved in exocytosis, and the relative orientation of these regions in the CTL membrane to the cleft which forms in the target cell membrane.

CTL Acquire Target Cell Membrane Protein and Form Membrane Bridges with the Targets

During these studies, we made two unexpected but related observations. First, in both live (Supplemental Movie S1) and fixed cell studies (Figure 7) using P815 target cells expressing pEYFP-mem, we frequently observed that pEYFP-mem extends from this point over the CTL cell surface (Figures 7B and 7C and, especially strikingly, in Supplemental Movie S1). In addition, pEYFP-mem can also be seen in isolated CTL, suggesting that the protein expressed by P815 has been transferred to CTL (Figure 7A). Intriguingly, these CTL often have decreased levels of granule content marker, suggesting that they have already released some of their granules. In order to determine whether the transfer of membrane proteins is bidirectional, we stained conju-

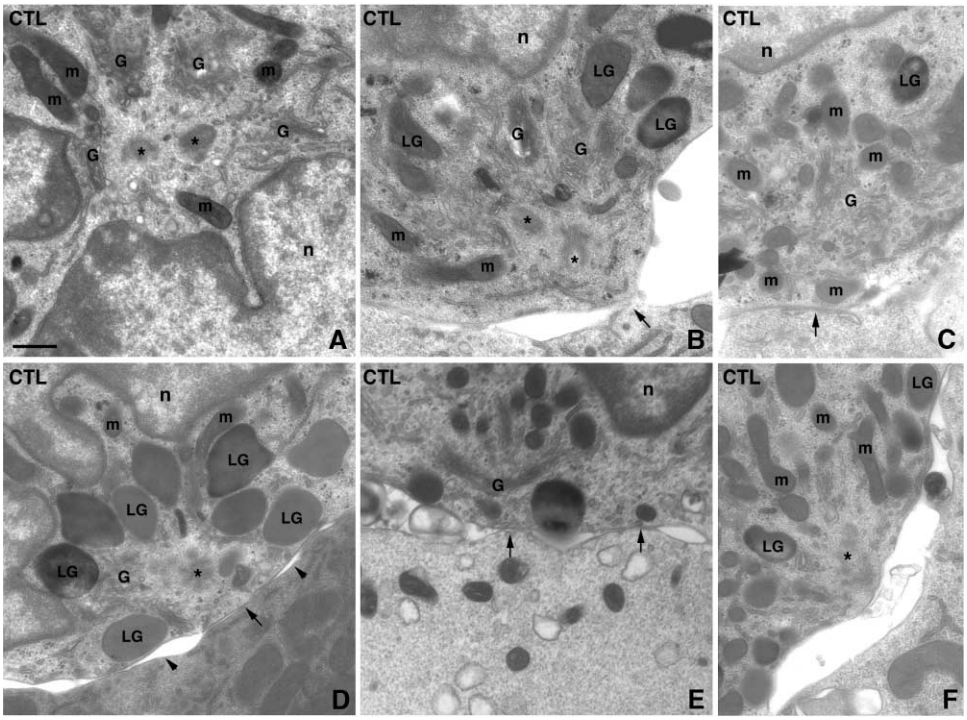

Figure 5. A Cleft Appears between the Two Cell Membranes Opposite the Site of Lysosome Secretion

Semithin (100–200 nm) stained sections of CTL loaded with HRP to identify secretory lysosomes in the absence of P815 targets (A) or after conjugation with P815 targets (B–F) showing events at the contact site at different stages of lysosome polarization and exocytosis (compare Figures 2A–2E). The two centrioles (asterisks) mark the position of the MTOC. Note that when LG are next to the plasma membrane, gaps between the otherwise tightly apposed cell membranes appear opposite aligned LG (arrowheads, [D]), into which the LG appear to release their content (E). Note that the LG never align directly opposite the MTOC/Golgi stack and that the membranes are in tight contact at this point (arrow, [D and E]). A section just below that of the most aligned Golgi stacks which reveals that the gaps form part of a large cleft between the two cells (F). m, mitochondria; n, nucleus; G, Golgi complex; LG, lytic granule. The scale bar represents 500 nm.

gates with antibodies to the MHC class I specific to the target, H2Dd (Figures 7D–7G) and CD8 specific to the CTL (Figures 7E–7G). These studies revealed that while H2Dd is acquired by CTL, CD8 is not transferred to the target cells. Figures 7E and 7F show two confocal sections through the same pair of cells after a 2 hr

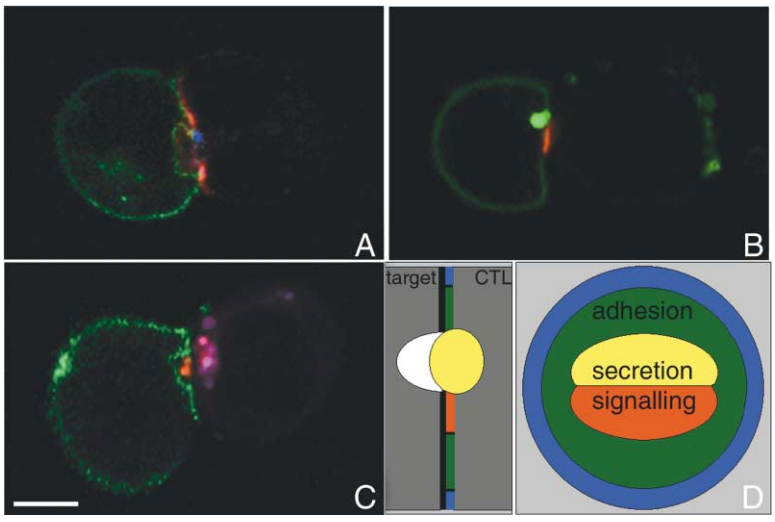

Figure 6. The Cleft Appears as an Indentation in the P815 Target Cell Membrane Opposite the Site of Granule Secretion

(A–C) CTL (right) conjugated to P815-pEYFP-mem target cells (left; green) prepared as described in Figure 2. In (A) is shown talin (red) granzyme A (blue); in (B), Lck (red); and in (C), granzyme A (red) and cathepsin D (blue). The cleft between the cells can be seen as an indentation into the target cell encircled by the talin ring, which contains granule content. (D) A model showing the arrangement of proteins and structures at the CTL-target cell contact site as seen in section through the cell-cell contact site (left) and looking flat down onto the contact site on the side of CTL (right). The adhesion molecules (green) form a ring of tight membrane:membrane contact surrounding two separate and distinct domains, one containing the signaling proteins (red) and one which is opposite a gap between the otherwise tightly associated membranes and at which the LG polarize, align, and secrete their content (yellow). The ring shown in blue represents proteins that are excluded from the contact site. The scale bar represents 4 μm.

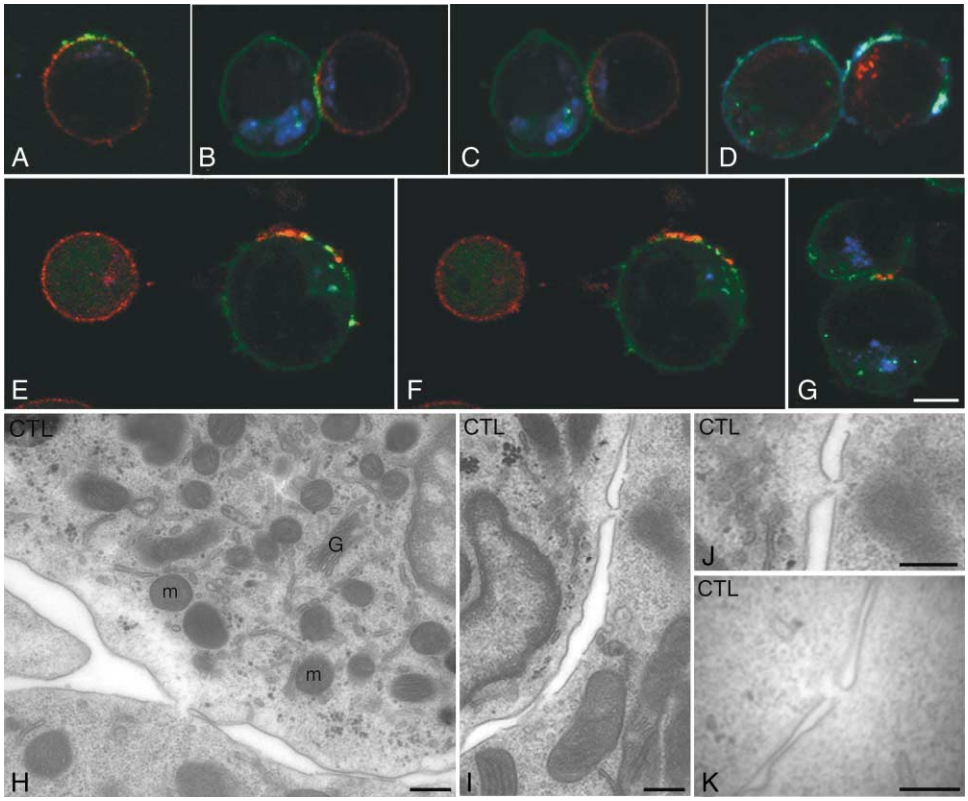

Figure 7. As CTL Detach, Membrane Transfers from the Target to the CTL and Membrane Bridges Are Observed between the Two Cell Membranes

(A–F) Confocal images showing CTL after detachment (A) or in the process of detaching from P815-pEYFP-mem (B–D) or P815 (E and F) target cells, fixed and labeled with antibodies against cathepsin D (blue) and Lck (red) (A–C); granzyme A (red) and H2Dd (blue) (D); H2Dd (red), CD8 (green), and cathepsin D (blue) (E and F). All cells were conjugated for 30 min except for in (E) and (F), which were incubated for 120 min prior to fixation. (B) and (C), and (E) and (F) represent two separate section planes through the same pairs of cells.

(G) A conjugate is shown formed between two CTL labeled with CD8 (green), H2Dd (red), and cathepsin D (blue). The granules in the upper cell are polarizing toward the lower cell with H2Dd at the interface.

(H–K) Semithin (~100 nm) stained sections of CTL loaded with HRP to label the lytic granules and in the process of detaching from their targets are shown. Note the disorganized arrangement of the organelles and the absence of LG from the contact site in the detaching CTL (H). Additional examples of sites of membrane:membrane fusion on CTL-target cell detachment are shown in (I–K). (J) is a higher magnification of (I). m, mitochondria; n, nucleus; G, Golgi complex. The scale bars represent 4 μm in (A–G) and 250 nm in (H–K).

conjugation. These images reveal long processes extending from the target to CTL, with H2Dd tightly associated or incorporated into the plasma membrane of the CTL. Remarkably, conjugates can also be found between two CTL with H2Dd at the interface and the granules of one CTL polarized toward the other (Figure 7G), suggesting that acquisition of H2Dd is leading to CTL recognition by CTL (fratricide).

The second observation was from EM images of conjugates that were in the process of separating. These cells can be identified because the MTOC and cytoplasmic organelles in the CTL are not tightly polarized toward the target cell but have a random and disorganized arrangement, and the two cell membranes are largely separated (Figures 7H and 7I). However, some points of contact remain, and high magnification images of these contact sites (Figures 7J and 7K) reveals them to be points at which the two cell membranes have fused together to form membrane bridges, creating channels with a central diameter ranging between ~50 and 95 nm. Tilting of semithick (200–500 μm) sections at high magnification over a range between −45° and +45° confirms that the two cell membranes are continuous at these points (data not shown). Fusion of the CTL and target cell membranes appears to occur independently of granule exocytosis, since it is also observed using CTL derived from patients with genetic defects preventing secretion. For example, in CTL derived from patients with Chediak-Higashi syndrome, in which the granules can polarize but are unable to secrete their content (Baetz et al., 1995), membrane fusion is also observed at the immunological synapse (J.C.S. and G.M.G., unpublished data). This data raises the possibility that the transfer of both pEYFP-mem and H2Dd from the target cell to the CTL may occur by transfer of membrane at these points of fusion.

Discussion

Although it has long been known that the granules polarize to the site of membrane contact between CTL and target (Peters et al., 1989; Yannelli et al., 1986), neither

the molecular arrangement nor the precise site of granule secretion has been described. In this paper, we show that, despite the rapid killing of targets by CTL, an immunological synapse is formed between the two cells. The granules are secreted at a specific site within the adhesion ring, distinct from the signaling region of the immunological synapse. Granule polarization and secretion occur opposite a cleft, which is formed by indentation of the target cell membrane. Our studies also reveal that direct membrane fusion between CTL and target occurs as a result of synapse formation and that the CTL acquires membrane proteins from the target.

The overall structure of the CTL synapse is very similar to that described for CD4 cells engaged with APCs, with adhesion molecules in a ring surrounding the signaling molecules (Monks et al., 1998). When a CTL is engaged in killing a target, we find that CD11a and talin colocalize in the pSMAC, while Lck and PKC-θ cluster in the cSMAC. CD3ζ is also localized in the cSMAC (data not shown), while CD45 appears to be excluded from the synapse. We have also shown that the actin-polymerizing complex Arp2/3 localizes to the center of the talin hole (Stinchcombe et al., 2001), suggesting that some actin may be present although inaccessible to antibody or phalloidin. The major difference between the CD8 and CD4 synapses is the presence of a distinct secretory domain within the pSMAC of CD8 cells conjugated to their targets. It is possible that a secretory domain exists within the CD4 synapse but has simply not been detected yet. Studies on CD4 cells showing that ionomycin treatment increases cell surface expression of secretory lysosomal proteins CD63 and Fas ligand within 5 min (Bossi and Griffiths, 1999) support the idea that these secretory organelles are present in CD4 cells. Interestingly, the CTL synapse differs from that described for an NK cell receiving a negative NK receptor signal where the adhesion molecules appear to be surrounded by the signaling molecules (Davis et al., 1999). It remains to be seen whether the NK synapse adopts a CTL-like structure upon receiving a positive signal which causes granule secretion.

By comparing the degree of granule polarization and synapse formation by both light (Figure 2) and electron (Figure 5) microscopy, we have been able to order these events relative to one another. It should be emphasized that the CTL used are an allogeneic cell line (generated after three rounds of stimulation in vitro) and the conjugates formed will vary both in strength of TCR recognition and length of time conjugated. Previous studies have demonstrated that the MTOC and Golgi complex polarize before the granules. We also observe that the plasma membranes between the two cells form an extensive area of tight contact, and the adhesion ring is smaller in diameter when the granules are polarized (Figures 5C and 2H–J). When the granules are docked at the membrane, a cleft is apparent within this region of tight contact (Figure 5D). The granules dock preferentially at the membrane opposite these clefts and secrete their contents into them (Figure 5E). Taken together, these findings show that secretion occurs within a defined region of this synapse, indicating that synapse structure is important in directing secretion.

Several interesting points emerge from defining the site of granule secretion. First, secretion only occurs after the membranes of the two cells have formed a very tight seal between the cells. Given the potency of the lytic proteins perforin and Fas ligand, this is likely to be important in limiting exposure of these proteins to the target cell recognized. Second, the granules polarize and dock at a specific site defined by a cleft between the otherwise tightly apposed membranes of the two cells. Curiously, the cleft seems to be formed by indentation of the target cell membrane (Figures 1D and 6). Interestingly, these clefts have been seen before in EM studies of CTL-target conjugates (Bykovskaja et al., 1978a, 1978b; Geiger et al., 1982; Sanderson and Glauert, 1979). We do not know what triggers cleft formation or why the granules should dock and fuse at this site, but it is clear that cleft formation is independent of secretion as it is also seen in the synapses formed by mutant CTL that cannot secrete their granules (Stinchcombe et al., 2001).

Another point of interest is that the areas of tight membrane contact and the organization of signaling proteins are both maintained during secretion. This suggests that signaling can be maintained while secretion is occurring. Previous studies have shown that TCR signaling in CTL not only stimulates secretion, but also results in the synthesis of new lytic proteins, which can refill the granules (Isaaz et al., 1995). Therefore, sustained signaling during secretion may well be important in facilitating serial killing by CTL. Our results also suggest that serial killing may not always require new synthesis of lytic proteins. The time-lapse video microscopy shows that only a proportion of the LysoTracker-labeled granules needs to be released in order to initiate signs of target cell death (Supplemental Movie S1). This suggests that only a small number of granules need to release their contents in order for a CTL to kill a target. We frequently observe the same CTL going on to kill subsequent targets. This indicates that CTL can then go on to establish new contacts, and polarize and release the content of further granules in order to continue killing.

Perhaps the biggest surprise of these studies was what happens at late stages of CTL killing. We observe both transfer of membrane proteins from the targets to CTL and direct membrane fusion between CTL and target at the area of contact. Our finding that isolated CTL carrying membrane proteins of the target cells are observed with time in both live and fixed cell studies is very reminiscent of recent reports of antigen transfer from target to CTL (Huang et al., 1999; Hudrisier et al., 2001) and from APCs to B cells, which also form synapses (Batista et al., 2001). Interestingly, MHC class I transfer to CTL has been shown to be antigen dependent, indicating that TCR recognition and synapse formation are required. Furthermore, acquisition of antigen renders the recipient CTL susceptible to lysis by other CTL (fratricide; Huang et al., 1999).

Could another function of synapse formation be to allow CTL to gradually acquire antigen with each successive target killed? In this way, CTL which have killed multiple targets will themselves be recognized and destroyed by other CTL (fratricide), and the CTL response will be downregulated as the targets are killed. Our findings are entirely consistent with this scheme and suggest that unidirectional membrane transfer can occur

during synapse formation (Figures 7B–7F) and can lead to CTL recognition of CTL (Figure 7G). Curiously, EM of conjugates with tightly apposed membranes often reveals points of direct membrane fusion between CTL and target. These "bridges" are only seen at dissolving synapses where the organelles have lost the tight polarization and the cells are slightly parted. It is difficult to quantitate the frequency of these bridges. However, they are observed more frequently than a granule releasing its contents (Figure 5E). We do not see bridges in CTL which are tightly apposed in the absence of TCR recognition. One possibility is that these membrane bridges are the result of synapse formation and that transfer of membrane proteins occurs by virtue of these continuities. Taken together, these observations suggest, but do not prove, that the transfer of membrane proteins from target to CTL may occur as a consequence of membrane fusion between the two cells leading to the CTL ripping off the membrane of the compromised target as they part. The recent report by Hudrisier et al. demonstrates that CTL acquire not only MHC class I, but also several other membrane proteins as well as lipids from the target cell (Hudrisier et al., 2001), supporting a role for membrane ripping. Furthermore, the images shown in Figures 7E and 7F are suggestive of membrane under tension, as the cells part.

The attractive side of these observations is that with every target killed, the CTL acquires more antigen, increases its chance of being killed by fratricide, and provides a self-regulating mechanism for turning off the CTL response. There is, however, a distinctly unattractive side to a membrane fusion, which results in the formation of large channels (50–90 nm) between CTL and target. CTL destroy their targets by delivering granzymes from the lytic granules into the cytoplasm of the target cell (Lowin et al., 1995). Although there is currently some controversy about whether this delivery takes place at the plasma membrane or from an endosome within the target (Motyka et al., 2000), it is clear that the granzymes act on caspases in the target cell cytoplasm which trigger apoptosis (reviewed in Darmon and Bleackley, 1998; Page et al., 1998). Do these channels allow granzymes secreted by the CTL into the target back into the CTL? In preliminary studies, we have been unable to detect transfer of either GFP or CFSE from the cytoplasm of the target to that of the CTL, or CFSE from the CTL to the target. It is possible that these methods are not sensitive enough to detect transfer. However, since CTL which have acquired the EYFP-mem marker are clearly viable and able to continue their effector function, this supports the idea that if transfer occurs, it is too little to effect CTL cell death.

The studies reported here reveal that CTL do form immunological synapses with their targets. Within these synapses, granule secretion occurs within a defined domain. One consequence of synapse formation appears to be direct fusion of the plasma membranes between CTL and target. This provides a mechanism for the transfer of antigen from target to CTL with progressive killing. Taken together, these findings suggest that the structure of the immunological synapse is important not only in signaling, but also in the polarized secretion which mediates target destruction and the transfer of antigen which mediates downregulation of the CTL response.

Experimental Procedures

Antibodies

A rabbit antiserum against actin, mouse monoclonal antibodies recognizing talin, and the *cis*-Golgi 58 kDa protein (p58), and FITC-conjugated rat monoclonal antibodies against mouse CD11a and mouse CD45 were all obtained from Sigma-Aldrich. Mouse and rat monoclonal antibodies against Lck and tubulin, respectively, were from Chemicon International, and mouse monoclonal antibodies recognizing PKC-θ were from Transduction Laboratories, and H2Dd was from Pharmingen. The rabbit antiserum against cathepsin D and rat monoclonal recognizing granzyme A (7.1) (Fruth et al., 1987) were generous gifts of S. Kornfeld (Washington University, St. Louis, MO) and M. Simon (Max-Planck-Institute, Freiburg, Germany), respectively. Secondary antibodies conjugated to Cy3, Cy5, Texas red, and FITC were all obtained from Jackson ImmunoResearch Laboratories.

Cell Preparation and Culture

Single-cell suspensions of mouse splenocytes from C57BL/6, 129Sv/Ev, or BALB/c mice were generated by passing cells through a 70 μm nylon strainer (Becton Dickinson). 2.5×10^7 responders were mixed with an equal number of BALB/c-derived stimulators (irradiated at 3000 Rad) in 10 ml Iscove's modified Dulbecco's medium (IMDM) supplemented with 10% FCS, 50 μM 2-mercaptoethanol, and 100 U/ml IL-2 (Gibco) and 50 U/ml penicillin and streptomycin (Gibco). After 5 days, CTL cells were purified by separation over Ficoll Histopaque 1083-1 (Sigma-Aldrich), washed three times in IMDM, 10% FCS, and resuspended in culture medium as above at a density of approximately 10^6 cells/ml. $2–5 \times 10^6$ CTL were restimulated at 7–10 days after stimulation with 2.5×10^7 irradiated stimulators up to six times after the initial stimulation.

P815 mouse target cells were maintained in RPMI, 10% FCS. To obtain clonal P815 target cells expressing the EYFP-tagged palmitoylation domain of neuromodulin (pEYFP-mem; Clontech), 4×10^6 cells were washed and resuspended in RPMI lacking serum. Twenty-five micrograms of pEYFP-mem DNA was added, mixed, and incubated for 10 min at room temperature before electroporation at 270 V and 500 μF. Samples were left a further 10 min and then transferred to 5 ml of complete medium (RPMI, 10% FCS) and incubated for 24 hr before adding 1 mg/ml G418. After 6 days of selection, the cells were cloned by limiting dilution in selection medium and cells expressing the membrane marker were referred to as P815-pEYFP-mem.

Live Cell Video Microscopy

C57BL/6 CTL were incubated with 60 nM LysoTracker Red DND-99 (Molecular Probes) for 2 hr at 37°C in RPMI, 10% FCS and then washed three times in PBS and resuspended in 100 μl of RPMI, 10% FCS. P815-pEYFP-mem target cells were allowed to adhere on a glass coverslip mounted in a temperature-controlled chamber for 10 min at 37°C in RPMI without serum. FCS was then restored to the medium to a final concentration of 10% and the LysoTracker Red DND-99-loaded CTL were added to the P815-pEYFP-mem in the chamber. Sequential confocal images were acquired every 10 s after the CTL had established contact with a target. A Nikon TE300 microscope attached to a Bio-Rad Radiance2000 MP laser scanning microscope was used, with a 488 nm and a 543 nm laser for epifluorescence and Nomarski differential interference contrast for the transmitted light. The images were processed using MetaMorph version 4.5 software.

Immunofluorescence

C57BL/6 and 129Sv/Ev CTL taken 5–8 days after stimulation and P815 or P815-pEYFP-mem target cells were washed in RPMI, and each cell pellet was resuspended to a final concentration of $\sim 5 \times 10^6$ cells/ml in RPMI. CTL and target cells were mixed 1:1, left for 5 min in suspension, and then plated onto glass multiwell slides and incubated at 37°C for 30–120 min. Samples were fixed for 5 min with methanol precooled to −20°C, washed extensively in PBS, blocked in PBS, 1% BSA (Sigma-Aldrich), and processed for immunofluorescence. Primary antibodies were added in the presence of 1% BSA for 45 min and washed extensively in PBS, 1% BSA (Stinchcombe et al., 2000). Secondary antibodies were added in the

presence of 1% BSA for 30–40 min, washed extensively in PBS, 1% BSA and then in PBS and mounted in PBS containing 90% glycerol and 2.5% DABCO. Samples were examined using either an MRC-1024 Bio-Rad laser scanning confocal microscope and with the iris set at 1.4 or a Bio-Rad Radiance2000 MP laser scanning microscope, with lasers exciting at 488, 543, and 638 nm. Three-dimensional (3D) images are shown represented as both single composites in Figure 4 and Supplemental Figure S1 and as 3D reconstructions in Supplemental Movies S2–S7. For 3D and z axis image reconstruction, 40 (Figure 4B) or 30 (Figure 4F) confocal sections, 0.4 μm apart, were taken and assembled using MetaMorph Version 4.5 software. Z axis image reconstruction over the contact area was carried out using the 3D ortholog function of MetaMorph version 4.5. Forty conjugates were counted using CTL from C57BL/6 conjugated to P815 targets for 30 min and stained for either Lck and cathepsin D or granzyme A and talin.

Electron Microscopy

C57BL6/J taken 5–8 days after stimulation were incubated overnight at 37°C with 2 mg/ml HRP (Boehringer Mannheim) added directly to the growth medium. Cells were washed approximately three times in RPMI and the final cell pellet was resuspended to a final concentration of $\sim 5 \times 10^6$ cells/ml in RPMI, and 500 μl aliquots were mixed 1:1 with RPMI alone or containing P815 target cells (prewashed in RPMI and also resuspended at $\sim 5 \times 10^6$ cells/ml in RPMI). After 5 min in suspension, samples were plated into individual wells of 12-well plastic tissue culture plates (Nunc). Conjugates were incubated for a further 30–55 min at 37°C, then fixed for 10–20 min by adding 1 ml of PBS containing 2× fixative (3% glutaraldehyde [Agar Scientific] and 4% paraformaldehyde [Electron Microscopy Sciences] directly to the incubation medium. Samples were incubated with fresh 1× fixative (1.5% glutaraldehyde and 2% paraformaldehyde in PBS) for a further 10 min, then washed with PBS and processed for DAB cytochemistry, postfixation with reduced osmium, and Epon embedding as described previously (Stinchcombe et al., 2000). Semi-thick (100–300 nm) samples were contrasted with lead citrate and examined using a Zeiss 912 Omega Electron Microscope.

Acknowledgments

This work is supported by a Wellcome Trust Senior Fellowship to G.M.G. (040825) and a JIF grant from the Wellcome Trust (057227). We would like to thank Gideon Berke, Jim Kaufman, Thomas Harder, and Anton van de Merwe for helpful discussions and critical reading of the manuscript, and Stuart Kornfeld and Markus Simon for antibodies to cathepsin D and granzyme A, respectively. In addition, we would like to thank Nick White for help in setting up live cell and 3D imaging and Lance Tomlinson for patient reproduction of the figures.

Received August 13, 2001; revised October 19, 2001.

References

Baetz, K., Isaaz, S., and Griffiths, G.M. (1995). Loss of cytotoxic T lymphocyte function in Chediak-Higashi syndrome arises from a secretory defect that prevents lytic granule exocytosis. J. Immunol. *154*, 6122–6131.

Batista, F.D., Iber, D., and Neuberger, M.S. (2001). B cells acquire antigen from target cells after synapse formation. Nature *411*, 489–494.

Bossi, G., and Griffiths, G.M. (1999). Degranulation plays an essential part in regulating cell surface expression of Fas ligand in T cells and natural killer cells. Nat. Med. *5*, 90–96.

Burkhardt, J.K., Hester, S., Lapham, C.K., and Argon, Y. (1990). The lytic granules of natural killer cells are dual-function organelles combining secretory and pre-lysosomal compartments. J. Cell Biol. *111*, 2327–2340.

Bykovskaja, S.N., Rytenko, A.N., Rauschenbach, M.O., and Bykovsky, A.F. (1978a). Ultrastructural alteration of cytolytic T lymphocytes following their interaction with target cells. I. Hypertrophy and change of orientation of the Golgi apparatus. Cell. Immunol. *40*, 164–174.

Bykovskaja, S.N., Rytenko, A.N., Rauschenbach, M.O., and Bykovsky, A.F. (1978b). Ultrastructural alteration of cytolytic T lymphocytes following their interaction with target cells. II. Morphogenesis of secretory granules and intracellular vacuoles. Cell. Immunol. *40*, 175–185.

Darmon, A.J., and Bleackley, R.C. (1998). Proteases and cell-mediated cytotoxicity. Crit. Rev. Immunol. *18*, 255–273.

Davis, S.J., and van der Merwe, P.A. (2001). The immunological synapse: required for T cell receptor signalling or directing T cell effector function? Curr. Biol. *11*, R289.

Davis, D.M., Chiu, I., Fassett, M., Cohen, G.B., Mandelboim, O., and Strominger, J.L. (1999). The human natural killer cell immune synapse. Proc. Natl. Acad. Sci. USA *96*, 15062–15067.

Delon, J. (2000). The immunological synapse. Curr. Biol. *10*, R214.

Delon, J., and Germain, R.N. (2000). Information transfer at the immunological synapse. Curr. Biol. *10*, R923–R933.

Fruth, U., Prester, M., Golecki, J.R., Hengartner, H., Simon, H.G., Kramer, M.D., and Simon, M.M. (1987). The T cell-specific serine proteinase TSP-1 is associated with cytoplasmic granules of cytolytic T lymphocytes. Eur. J. Immunol. *17*, 613–621.

Geiger, B., Rosen, D., and Berke, G. (1982). Spatial relationships of microtubule-organizing centers and the contact area of cytotoxic T lymphocytes and target cells. J. Cell Biol. *95*, 137–143.

Grakoui, A., Bromley, S.K., Sumen, C., Davis, M.M., Shaw, A.S., Allen, P.M., and Dustin, M.L. (1999). The immunological synapse: a molecular machine controlling T cell activation. Science *285*, 221–227.

Huang, J.F., Yang, Y., Sepulveda, H., Shi, W., Hwang, I., Peterson, P.A., Jackson, M.R., Sprent, J., and Cai, Z. (1999). TCR-mediated internalization of peptide-MHC complexes acquired by T cells. Science *286*, 952–954.

Hudrisier, D., Riond, J., Mazarguil, H., Gairin, J.E., and Joly, E. (2001). Cutting edge: CTLs rapidly capture membrane fragments from target cells in a TCR signaling-dependent manner. J. Immunol. *166*, 3645–3649.

Isaaz, S., Baetz, K., Olsen, K., Podack, E., and Griffiths, G.M. (1995). Serial killing by cytotoxic T lymphocytes: T cell receptor triggers degranulation, re-filling of the lytic granules and secretion of lytic proteins via a non-granule pathway. Eur. J. Immunol. *25*, 1071–1079.

Kupfer, A., and Dennert, G. (1984). Reorientation of the microtubule-organizing center and the Golgi apparatus in cloned cytotoxic lymphocytes triggered by binding to lysable target cells. J. Immunol. *133*, 2762–2766.

Kupfer, A., and Singer, S.J. (1989). Cell biology of cytotoxic and helper T cell functions: immunofluorescence microscopic studies of single cells and cell couples. Annu. Rev. Immunol. *7*, 309–337.

Kupfer, A., Dennert, G., and Singer, S.J. (1985). The reorientation of the Golgi apparatus and the microtubule-organizing center in the cytotoxic effector cell is a prerequisite in the lysis of bound target cells. J Mol. Cell. Immunol. *2*, 37–49.

Kupfer, A., Singer, S.J., and Dennert, G. (1986). On the mechanism of unidirectional killing in mixtures of two cytotoxic T lymphocytes. Unidirectional polarization of cytoplasmic organelles and the membrane-associated cytoskeleton in the effector cell. J. Exp. Med. *163*, 489–498.

Lowin, B., Peitsch, M.C., and Tschopp, J. (1995). Perforin and granzymes: crucial effector molecules in cytolytic T lymphocyte and natural killer cell-mediated cytotoxicity. Curr. Top. Microbiol. Immunol. *198*, 1–24.

Matter, A. (1979). Microcinematographic and electron microscopic analysis of target cell lysis induced by cytotoxic T lymphocytes. Immunology *36*, 179–190.

Monks, C.R., Freiberg, B.A., Kupfer, H., Sciaky, N., and Kupfer, A. (1998). Three-dimensional segregation of supramolecular activation clusters in T cells. Nature *395*, 82–86.

Motyka, B., Korbutt, G., Pinkoski, M.J., Heibein, J.A., Caputo, A., Hobman, M., Barry, M., Shostak, I., Sawchuk, T., Holmes, C.F., et al. (2000). Mannose 6-phosphate/insulin-like growth factor II receptor is

a death receptor for granzyme B during cytotoxic T cell-induced apoptosis. Cell *103*, 491–500.

Page, L.J., Darmon, A.J., Uellner, R., and Griffiths, G.M. (1998). L is for lytic granules: lysosomes that kill. Biochim. Biophys. Acta *1401*, 146–156.

Peters, P.J., Geuze, H.J., Van der Donk, H.A., Slot, J.W., Griffith, J.M., Stam, N.J., Clevers, H.C., and Borst, J. (1989). Molecules relevant for T cell-target cell interaction are present in cytolytic granules of human T lymphocytes. Eur. J. Immunol. *19*, 1469–1475.

Peters, P.J., Borst, J., Oorschot, V., Fukuda, M., Krahenbuhl, O., Tschopp, J., Slot, J.W., and Geuze, H.J. (1991). Cytotoxic T lymphocyte granules are secretory lysosomes, containing both perforin and granzymes. J. Exp. Med. *173*, 1099–1109.

Poenie, M., Tsien, R.Y., and Schmitt-Verhulst, A.M. (1987). Sequential activation and lethal hit measured by [Ca2+]i in individual cytolytic T cells and targets. EMBO J. *6*, 2223–2232.

Rothstein, T.L., Mage, M., Jones, G., and McHugh, L.L. (1978). Cytotoxic T lymphocyte sequential killing of immobilized allogeneic tumor target cells measured by time-lapse microcinematography. J. Immunol. *121*, 1652–1656.

Sanderson, C.J. (1976). The mechanism of T cell mediated cytotoxicity. II. Morphological studies of cell death by time-lapse microcinematography. Proc. R. Soc. Lond. B. Biol. Sci. *192*, 241–255.

Sanderson, C.J., and Glauert, A.M. (1979). The mechanism of T-cell mediated cytotoxicity. VI. T-cell projections and their role in target cell killing. Immunology *36*, 119–129.

Stinchcombe, J.C., Page, L.J., and Griffiths, G.M. (2000). Cytotoxic T lymphocytes as a model system for studying secretory lysosome biogenesis. Traffic *1*, 435–444.

Stinchcombe, J.C., Barral, D.C., Mules, E.H., Booth, S., Hume, A.N., Machesky, L.M., Seabra, M.C., and Griffiths, G.M. (2001). Rab27a is required for regulated secretion in cytotoxic T lymphocytes. J. Cell Biol. *152*, 825–834.

Yannelli, J.R., Sullivan, J.A., Mandell, G.L., and Engelhard, V.H. (1986). Reorientation and fusion of cytotoxic T lymphocyte granules after interaction with target cells as determined by high resolution cinemicrography. J. Immunol. *136*, 377–382.

Zagury, D., Bernard, J., Thierness, N., Feldman, M., and Berke, G. (1975). Isolation and characterisation of individual functionally reactive cytotoxic T lymphocytes: conjugation, killing and recycling at the single cell level. Eur. J. Immunol. *5*, 818–822.